ORIGINAL ARTICLE

Emir Q. Haxhija · Hua Yang · Ariel U. Spencer
Xiaoyi Sun · Daniel H. Teitelbaum

Influence of the site of small bowel resection on intestinal epithelial cell apoptosis

Abstract Massive small bowel resection (SBR) results in a significant increase in intestinal epithelial cell (EC) proliferation as well as apoptosis. Because the site of SBR (proximal (P) vs. distal (D)) affects the degree of intestinal adaptation, we hypothesized that different rates of EC apoptosis would also be found between P-SBR and D-SBR models. Wild-type C57BL/6J mice underwent: (1) 60% P-SBR, (2) 60% D-SBR, or (3) SHAM-operation (transaction–reanastomosis) at the mid-gut point. Mice were sacrificed after 7 days. EC apoptosis was measured by TUNEL staining. EC-related apoptotic gene expression including intrinsic and extrinsic pathways was measured with reverse transcriptase-polymerase chain reaction. Bcl-2 and bax protein expression were analyzed by Western immunobloting. Both models of SBR led to significant increases in villus height and crypt depth; however, the morphologic adaptation was significantly higher after P- SBR compared to D-SBR ($P < 0.01$). Both models of SBR led to significant increases in enterocyte apoptotic rates compared to respective sham levels; however, apoptotic rates were 2.5-fold higher in ileal compared to jejunal segments ($P < 0.01$). P-SBR led to significant increases in bax (pro-apoptotic) and Fas expression, whereas D-SBR resulted in a significant increase in TNF-α expression ($P < 0.01$). EC apoptosis seems to be an important component of intestinal adaptation. The significant difference in EC apoptotic rates between proximal and distal intestinal segments appeared to be due to utilization of different mechanisms of action.

E. Q. Haxhija
Department of Pediatric Surgery,
Medical University Graz, Graz, Austria

H. Yang · A. U. Spencer · X. Sun · D. H. Teitelbaum (✉)
Section of Pediatric Surgery, Department of Surgery,
University of Michigan Medical School,
and C. S. Mott Children's Hospital, Mott F 3970,
P.O. Box 0245, Ann Arbor, MI 48109, USA
E-mail: dttlbm@umich.edu

Introduction

Short bowel syndrome (SBS) is characterized by maldigestion and malabsorption after extensive loss of the small bowel [1, 2]. In the rodent model of massive small bowel resection (SBR), the residual small intestine (both jejunum and/or ileum) undergoes a series of adaptive processes leading to a significant increase in intestinal absorptive surface area which reflects regulatory processes for reestablishment of the nutritional homeostasis of the body, the exact mechanisms of which are still poorly understood [3–5].

The degree of intestinal adaptation has been shown to depend on the amount of the resected tissue and also on the site of intestinal resection [6–8]. Distal small bowel has been shown to have a higher ability of adaptation compared to the proximal small bowel, i.e., ileum shows a greater postresectional adaptation than jejunum [7, 8]. Thus, a number of studies focused mainly on the investigation of the mechanisms that drive the ileal postresectional adaptation. However, others reported that both ileum and jejunum show similar morphologic adaptive responses [9] and that it is the jejunum that significantly augments its absorptive capacity after distal SBR (D-SBR), when compared to the ileum in a model of proximal SBR (P-SBR) [10].

Recently, increased rates of enterocyte apoptosis have been reported after massive SBR, indicating that not only crypt cell proliferation, but also enterocyte apoptosis may play the crucial role during the process of postresectional intestinal adaptation [11–13]. The importance of crypt cell apoptosis is elucidated by the fact that the death of one crypt cell may be responsible for the loss of more than 100 descendent crypt enterocytes [14].

So far, the mechanisms behind the potentially distinct adaptive responses of residual intestine after P-SBR

versus D-SBR remain elusive. The aim of this study was to investigate if differences in postresectional intestinal adaptation of jejunum and ileum may be related to differences in enterocyte apoptosis rates, as well as differences in gene and protein expression of the various apoptotic pathways [15].

Methods

Animals

Studies reported here conformed to the guidelines for the care and use of laboratory animals established by the University Committee on Use and Care of Animals at the University of Michigan (Ann Arbor, MI, USA) and protocols were approved by that committee. Male, specific pathogen-free C57BL/6J mice (The Jackson Laboratory, Bar Harbor, ME, USA) purchased at 8 weeks of age were housed in the animal care facility of the University of Michigan. Mice were maintained in a 12-h day–night rhythm at 23°C and a relative humidity of 40–60%.

Experimental design

To investigate the postresectional changes in the ileum versus jejunum, two different SBR models were utilized: (1) 60% P-SBR, resection of the small bowel between the point 2 cm distal to the ligament of Treitz and 10 cm proximal to the ileo-cecal junction, and (2) 60% D-SBR, resection of the small bowel between the point 10 cm distal to the ligament of Treitz and 2 cm proximal to the ileo-cecal junction. Small bowel transection (SHAM) and reanastomosis without bowel resection at the point approximately 14 cm distal to the ligament of Treitz was used as a sham operation. Each group was comprised of seven mice.

Surgical procedure

This procedure has been described previously [16]. Briefly, one day prior to surgery mice chow was exchanged to micro-stabilized rodent liquid diet (TestDiet, Richmond, IN, USA). Mice were anesthetized with pentobarbital sodium (50 mg/kg i.p.). Bowel end-to-end anastomoses were completed with interrupted 8–0 monofilament sutures. At the end of surgery, mice were resuscitated with a 3 ml subcutaneous injection of 0.9% saline solution. On the first postoperative day, mice were given only water and thereafter had free access to water and liquid diet [17]. Body weights were determined preoperatively and at harvest.

Harvesting

Mice were sacrificed at 7 days postoperatively using CO_2. The small bowel was exposed and 0.5 cm segments of small bowel were immediately immersed in 10% buffered formalin. Jejunal and ileal tissues were consistently taken from the sites 3 cm distal to the ligament of Treitz (D-SBR, SHAM-J) and 3 cm proximal to the ileo-cecal junction (P-SBR, SHAM-I), respectively. The parts of the small bowel 1 cm distal and 1 cm proximal to the anastomosis site were discarded. The remaining small bowel was immediately processed for mucosal cell isolation. The ileum or jejunum were harvested in the P-SBR and D-SBR groups, respectively. In the SHAM group the remaining ileum (SHAM-I) and jejunum (SHAM-J) were isolated separately.

Intestinal morphology and histology

Formaldehyde fixed tissues were dehydrated, embedded in paraffin, cut (5 μm thickness), and stained with H&E. Image Pro Plus Software (Media Cybernetics, Inc., Silver Spring, MD, USA) was used for measurements of villus height and crypt depth. Ten replicate measurements were made per tissue section and averaged.

Terminal deoxynucleotidyl transferase biotin–dUTP nick end labeling (TUNEL)

Jejunal and ileal paraffin-embedded tissues were assayed for apoptotic cells (broken DNA strands) by TUNEL staining (ApopTag Plus Peroxidase InSitu Apoptosis Detection Kit, Chemicon International Inc, Temecula, CA, USA), as previously described [16]. Slides were incubated with only one-third of the manufacturer's recommended concentration of TdT enzyme, in order to avoid over-staining.

Quantification of apoptosis

Assessment of apoptosis consisted of counting all TUNEL positive EC in all well-oriented crypts and villi separately and dividing the number of apoptotic cells per number of analyzed crypts and villi, respectively. Adding together of both crypt and villus apoptotic indices is expressed as the apoptotic index per crypt–villus complex. A Nikon TS-100 microscope was used at ×40 magnification and images were digitally recorded with an Evolution MP 5.1 CCD camera.

Mucosal cell isolation and purification

Mucosal cells were isolated and EC purified as previously described [18].

Reverse transcriptase-polymerase chain reaction (RT-PCR)

Total RNA was isolated using a guanidine isothiocyanate/chloroform extraction method using Trizol (Gibco BRL, Gaithersburg, MD, USA). EC mRNA (poly-A

positive) was reverse transcribed into cDNA following a standard protocol [19]. Specific primers for selected gene sequences of the members of the intrinsic (bcl-2, bax) and extrinsic (TNF-α, Fas) apoptotic pathways were designed using proprietary software (LaserGene, DNAStar, Inc, Madison, WI, USA). PCR and gel were run under standard conditions [20]. A Kodak EDAS System (Rochester, NY, USA) was used for imaging and quantification. Results were expressed as a ratio of the investigated mRNA over β-actin mRNA expression.

Immunoblot analysis

Protein concentration was determined using a Micro BCA Protein Assay Kit (Pierce Biotechnology Inc., Rockford, IL, USA). Approximately, 80 μg of total protein in loading dye was loaded per lane and separated on a SDS-polyacrylamide-gel electrophoresis (15%). Proteins were transferred to a PVDF membrane (Bio-Rad), treated with blocking solution (Zymed Laboratories, San Francisco, CA, USA) and probed overnight with either monoclonal mouse anti-bcl-2 antibody (1:400 in blocking solution; BD PharMingen, San Diego, CA, USA) or polyclonal rabbit anti-mouse bax antibody (1:1,000, in blocking solution, BD PharMingen). The membranes were then washed and incubated for 1 h at room temperature with either a 1:5,000 dilution of horseradish peroxidase (HRP)-conjugated goat anti-mouse IgG (Santa Cruz Biotechnology Inc., Santa Cruz, CA) or 1:8,000 HRP conjugated goat anti-rabbit IgG (Zymed Laboratories, San Francisco, CA, USA), respectively. Detection was done with enhanced chemiluminescence (Amersham) on X-OMAT AR film (Eastman Kodak, Rochester, NY, USA) and quantified using the same Kodak software mentioned above. Detection of β-actin was performed in the same fashion by re-probing membranes with purified anti-mouse β-actin (1:8,000, Sigma-Aldrich, St. Louis, MO, USA). The results are expressed as the ratio of target protein over β-actin protein expression.

Statistical analysis

All data are expressed as mean ± SD, unless indicated otherwise. The comparisons among groups were done using either student t test or one-way ANOVA followed by a Bonferroni t test for post hoc analysis of significance using Graph Pad Prism, Version 4.0 software (GraphPad, San Francisco, CA, USA). A value of $P < 0.05$ was considered significant.

Results

General description

All mice tolerated surgery well and showed no signs of intestinal obstruction at harvest. Seven days following SBR, body weight declined significantly in both SBR groups with a significantly higher body weight loss in the D-SBR group compared to P-SBR (percent change from weight at surgery: -15.5 ± 3 vs. $-9.9 \pm 3\%$, respectively, $P < 0.01$). There was no significant decline in body weight in SHAM operated mice.

Intestinal morphometric changes

The adaptive responses after SBR are shown in Table 1. Compared with the sham-transected group, villus height and crypt depth were significantly increased in both models of SBR 1 week after resection ($P < 0.001$); however, the relative increase in villus height was significantly higher after P-SBR than D-SBR (31 ± 4 vs. $18 \pm 7\%$, respectively; $P < 0.001$). Similarly, P-SBR resulted in a greater increase in crypt depth compared to the D-SBR group (35 ± 5 vs. $26 \pm 8\%$; $P < 0.05$).

Epithelial cell apoptosis

Enterocyte apoptosis rates were significantly higher in ileal segments compared to jejunum. Massive SBR caused a significant increase in EC apoptosis for both the D-SBR and P-SBR groups compared to the respective SHAM segments (Fig. 1). Interestingly, the rates of EC apoptosis were 2.5-fold higher in ileal segments (SHAM-I and P-SBR) compared to jejunal segments (SHAM-J and D-SBR).

Expression of apoptosis related genes and proteins

To investigate the mechanisms which resulted in the differences in EC apoptotic rates, several factors in both the intrinsic (bcl-2 family of proteins) and extrinsic (TNF-α and Fas) components of apoptotic signaling were studied. Results showed a significant increase in postresectional gene expression of bcl-2 after both SBR models compared to respective SHAM levels. Expression of bcl-2 was significantly higher after D-SBR compared to P-SBR ($P < 0.01$, Fig. 2). The expression of the pro-apoptotic gene bax increased significantly after P-SBR ($P < 0.05$), but did not change significantly after D-SBR ($P = $ns). Although bax-expression from SHAM segments was higher in jejunal compared to ileal segments ($P < 0.05$, Fig. 2), the bax to bcl-2 ratio was lower after D-SBR compared to P-SBR ($P < 0.05$, Table 2).

Western blot analysis confirmed the changes of bcl-2 and bax (Fig. 3). A significant increase in postresectional expression of bax was only found after P-SBR ($P < 0.05$). However, in SHAM segments, the expression of bax protein was consistently higher in jejunal compared to ileal segments ($P < 0.01$). On the other hand, bcl-2 protein expression showed a significant increase in both models of SBR compared to SHAM levels with a significantly higher expression in jejunal than ileal seg-

Table 1 Changes in villus height and crypt depth

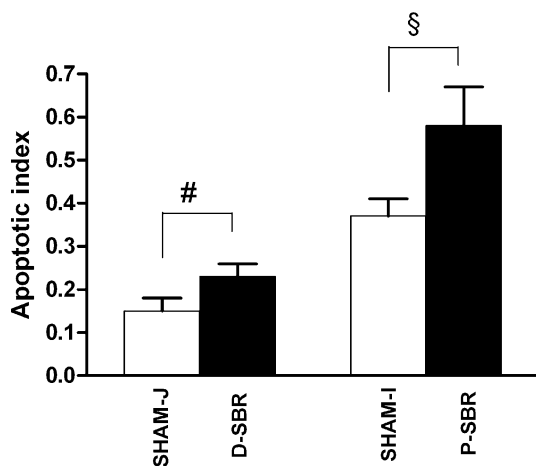|	Villus height (μm)	Crypt depth (μm)
SHAM-J	353 ± 24	97 ± 10
D-SBR	431 ± 25*	133 ± 11*
SHAM-I	229 ± 9	80 ± 4
P-SBR	332 ± 12*	121 ± 5*

The effects of distal (D) and proximal (P) small bowel resection (SBR) on changes in villus height and crypt depth at 7 days after surgery compared to sham transection (in jejunum and ileum (J and I, respectively) are shown. Values represent means ± SD. In each group $n = 7$ * $P < 0.001$

ments ($P < 0.01$, Fig. 3). This resulted in significantly lower bax to bcl-2 ratio after D-SBR compared to P-SBR ($P < 0.01$, Table 2).

Gene expression of the investigated members of the extrinsic apoptotic pathway (TNF-α and Fas) also showed marked segmental differences (Fig. 4). After P-SBR there was no change in the expression of TNF-α, but a significant increase in the expression of Fas compared to SHAM-I levels ($P < 0.05$). In contrast, when compared to SHAM-J after D-SBR, no change in Fas mRNA expression but a significant increase in the expression of TNF-α was found ($P < 0.05$). Interestingly, at SHAM-levels mRNA expression of Fas was significantly higher in jejunum compared to ileum and the opposite was the case for TNF-α ($P < 0.01$, respectively).

Discussion

This study showed that at 7 days after massive SBR in mice there is a marked difference in enterocyte apoptosis rates between proximal and distal small gut. A similar difference in baseline rates of apoptosis was also
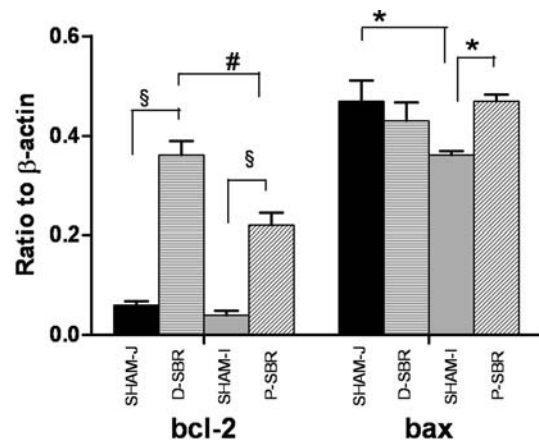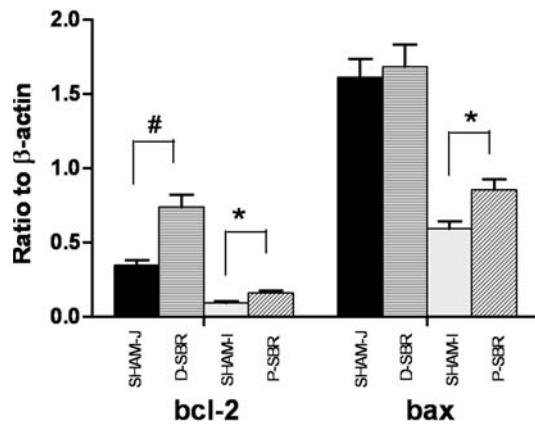

Fig. 2 mRNA expression of bcl-2 and bax at 7 days after distal and proximal SBR compared to respective segments of sham-transected mice. Note the significant increase in bcl-2 in both D-SBR and P-SBR groups, as well as the significantly higher levels of bcl-2 expression after D-SBR compared to P-SBR. Values represent means ± SD.* $P < 0.05$, § $P < 0.001$

observed when looking at SHAM operated mice. Additionally, P-SBR induced a higher morphologic intestinal adaptive response and was associated with a higher EC apoptotic rate compared to D-SBR. Finally, this difference in EC apoptotic rates after different sites of SBR may be due to the differential expression of the members of extrinsic and intrinsic apoptotic pathways along the proximal–distal small gut axis.
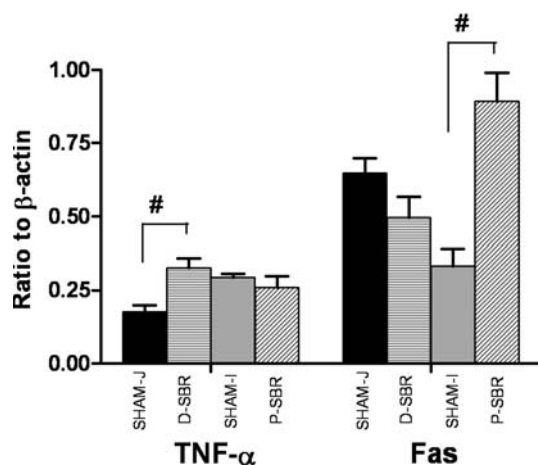
Intestinal adaptation after massive SBR is a complex process involving numerous nutritive and nonnutritive factors that lead to cellular hyperplasia and result in compensatory increases in villus height and crypt depth [1, 5, 18]. We set up our studies at 7 days postresection because it has been shown that in rodents, by this time-point, the majority of postresectional intestinal morphologic changes have been achieved [9]. Our findings of higher morphologic changes in the ileal segment compared to jejunal segment support previous reports showing that the ileum has a greater adaptive capacity to intestinal resection compared to the jejunum [6–8]. This phenomenon has been attributed to the increased load of chyme and intestinal secretions in the ileal segment after P-SBR. In our study, mice lost significantly less weight after P-SBR compared to D-SBR, which also suggests a greater adaptive capacity of ileum compared to jejunum.

Morphologic adaptation after SBR has been shown to be driven by changes in crypt cell proliferation and enterocyte apoptosis rates [11, 13, 21]. In the rapidly proliferating intestinal epithelium the ratio between enterocyte proliferation and apoptosis is responsible for maintenance, enhancement or loss of intestinal absorptive function [22]. Cell loss in the small intestine is mainly regulated by programmed cell death [23]. Several studies have recently shown that EC apoptosis is increased in the frame of intestinal adaptation after P-SBR, and emphasized that bax is the major protein

Fig. 1 Changes in the overall epithelial cell apoptosis rates (number of apoptotic cells per crypt–villus complex) at 7 days after SBR compared to sham transection are shown. Note the 2.5-fold higher enterocyte apoptotic rates in ileal compared to jejunal segments. Values represent means ± SD. In each group $n = 7$. # $P < 0.05$, § $P < 0.01$

Fig. 3 Protein expression of bcl-2 and bax at 7 days after distal and proximal SBR compared to respective segments of sham-transected mice. Note significantly higher bcl-2 levels after D-SBR compared to P-SBR and a significant increase in bax protein expression only after P-SBR. Values represent means ± SD. *$P < 0.05$, §$P < 0.001$

Table 2 Changes in bax to bcl-2 ratio

	Bax to bcl-2 ratio (mRNA)	Bax to bcl-2 ratio (Protein)
SHAM-J	7.8 ± 1.6	4.6 ± 1.4
D-SBR	1.2 ± 0.8**	2.3 ± 0.8*
SHAM-I	9 ± 1.7	6.3 ± 1.5
P-SBR	2.2 ± 0.5**	5.3 ± 1.8

Effects of distal (D) and proximal (P) small bowel resection (SBR) on changes in bax to bcl-2 ratio compared to respective sham levels. Both mRNA and protein data are shown at 7 days after surgery. Note significant decreases in mRNA bax to bcl-2 ratios in both SBR models and a significant decrease in protein bax to bcl-2 ratio only after D-SBR. Values represent means ± SD. In each group $n = 5$–7
*$P < 0.05$, **$P < 0.001$

that drives increased EC apoptosis after SBR [11, 24, 25]. On the other hand, others have also reported an increased expression of Fas, another potent inducer of apoptosis over the death receptor pathway after P-SBR [13]. This suggests that not only the bcl-2 family but also the members of the extrinsic apoptotic pathway are involved in regulation of postresectional EC apoptosis. Our results show that besides the significant increases in EC apoptosis rates at 7 days postsurgery in both SBR models, EC apoptosis rates per crypt/villus complex were significantly higher in ileal compared to jejunal segments. Analysis of gene and protein expression of selected members of intrinsic and extrinsic apoptotic pathways revealed that their expression profiles vary greatly along the proximal–distal axis of the gut. We found that after P-SBR, both bax and Fas gene

expression were up-regulated; and that these findings are supported by previous studies [11, 13]. However, tumor necrosis factor alpha (TNF-α) was the only factor found to be up-regulated at 7 days after D-SBR. TNF-α was also found to be up-regulated after mid-gut resection in mice [16]. This suggests that different mechanisms may be responsible for the regulation of apoptosis in ileal versus jejunal sections of the intestine.

Interestingly, analysis of bcl-2 expression showed that bcl-2 is highly up-regulated after SBR in both P-SBR and D-SBR models. Bcl-2 is an anti-apoptotic member of the bcl-2 family and has the capability to prevent cell death [26]. Furthermore, mice which were bcl-2 deficient had significantly shorter villi [27], whereas mice over-expressing bcl-2 showed increased intestinal adaptation compared to wild-type mice [28]. In addition, increased ratios between the pro-apoptotic and anti-apoptotic members of the bcl-2 family have been shown to create an environment favoring apoptosis [25, 29]. The up-regulation of bcl-2 after SBR, as found in our study, may indicate a higher resistance of intestinal EC to apoptosis during the process of postresectional intestinal adaptation. Possibly increased levels of bcl-2 and a lower postresectional bax to bcl-2 ratio may play an important protective role in intestinal adaptation following SBR (Table 2).

In conclusion, our data indicate that:

1. There are distinct adaptive responses upon SBR between proximal and distal small gut
2. Higher morphologic adaptation of ileum upon P-SBR is associated with higher rates of EC apoptosis compared to jejunum after D-SBR, indicating that increased cell growth is associated with an increased cell death
3. There is a differential expression of apoptosis related genes and proteins along the proximal to distal axis of the small intestine.

Fig. 4 Alterations in mRNA expression of Fas and TNF-α at 7 days after distal and proximal SBR compared to respective segments of sham-transected mice. Note the differential expression of TNF-α and Fas between the different sites of resection. Values represent means ± SD. *$P < 0.05$, #$P < 0.01$

References

1. Hoellwarth ME (1999) Short bowel syndrome: pathophysiological and clinical aspects. Pathophysiology 6:1–19
2. Williamson RCN (1984) Adaptive intestinal hyperplasia. In: Batt RM, Lawrence TLJ (eds) Function and dysfunction of the small intestine. Liverpool University Press, Liverpool, pp 55–76
3. Nygaard K (1967) Resection of the small intestine in rats. III. Morphological changes in the intestinal tract. Acta Chir Scand 133:233–248
4. Bristol JB, Williamson RCN (1988) Nutrition, operations and intestinal adaptation. JPEN J Parenter Enteral Nutr 12:299–309
5. Weale AR, Edwards AG, Bailey M, Lear PA (2005) Intestinal adaptation after massive intestinal resection. Postgrad Med J 81:178–184
6. Hansen WR, Osborne JW, Sharp JG (1977) Compensation by the residual intestine after intestinal resection in the rat. I. Influence of the amount of tissue removed. Gastroenterology 72:701–705
7. Weser E, Hernandez MH (1971) Studies of small bowel adaptation after intestinal resection in the rat. Gastroenterology 60:69–75
8. Appleton GVN, Bristol JB, Williamson RCN (1987) Proximal enterectomy provides a stronger systemic stimulus to intestinal adaptation than distal enterectomy. Gut 28:165–168
9. Juno RJ, Knott AW, Erwin CR, Warner BW (2003) A serum factor(s) after small bowel resection induces intestinal epithelial cell proliferation: effects of timing, site and extent of resection. J Pediatr Surg 38:868–874
10. Wang HT, Miller JH, Avissar N, Sax HC (1999) Small bowel adaptation is dependent on site of massive enterectomy. J Surg Res 84:94–100
11. Helmrath MA, Erwin CR, Shin CE, Warner BW (1998) Enterocyte apoptosis is increased following small bowel resection. J Gastroenterol 2:44–49
12. Thompson JS, Barent B (1999) Effects of intestinal resection on intestinal apoptosis. J Gastrointest Surg 3:672–677
13. Tang Y, Swartz-Basile DA, Swietlicki EA, Yi L, Rubin DC, Levin MS (2004) Bax is required for resection-induced changes in apoptosis, proliferation, and members of the extrinsic cell death pathways. Gastroenterology 126:220–230
14. Potten CS, Booth C, Pritchard DM (1997) The intestinal epithelial stem cell: the mucosal governor. Int J Exp Pathol 78:219–243
15. Green DR (2003) Overview: apoptotic signaling pathways in the immune system. Immunol Rev 193:5–9
16. Wildhaber BE, Yang H, Haxhija EQ, Spencer AU, Teitelbaum DH (2005) Intestinal intraepithelial lymphocyte derived angiotensin converting enzyme modulates epithelial cell apoptosis. Apoptosis (in press)
17. Helmrath MA, VanderKolk WE, Can G, Erwin CR, Warner BW (1996) Intestinal adaptation following massive small bowel resection in the mouse. J Am Coll Surg 183:441–449
18. Yang H, Antony PA, Wildhaber BE, Teitelbaum DH (2004) Intestinal intraepithelial lymphocyte $\gamma\delta$–T cell-derived keratinocyte growth factor modulates epithelial growth in the mouse. J Immunol 172:4151–4158
19. Kiristioglu I, Teitelbaum DH (1998) Alteration of the intestinal intraepithelial lymphocytes during total parenteral nutrition. J Surg Res 79:91–96
20. Yang H, Fan Y, Finaly R, Teitelbaum DH (2003) Alteration of intestinal intraepithelial lymphocytes after massive small bowel resection. J Surg Res 110:276–286
21. Welters CFM, Dejong CHC, Deutz NEP, Heineman E (2002) Intestinal adaptation in short bowel syndrome. ANZ J Surg 72:229–236
22. Hall PA, Coates PJ, Ansari B, Hopwood D (1994) Regulation of cell number in the mammalian gastrointestinal tract: the importance of apoptosis. J Cell Sci 107:3569–3577
23. Potten CS (1997) Epithelial cell growth and differentiation. II. Intestinal apoptosis. Am J Physiol 273:G253–G257
24. Stern LE, Huang F, Kemp JC, Falcone RA, Erwin CR, Warner BW (2000) Bax is required for increased enterocyte apoptosis after massive small bowel resection. Surgery 128:165–170
25. Stern LE, Falcone RA, Huang F, Kemp JC, Erwin CR, Warner BW (2000) Epidermal growth factor alerts the bax:bcl-w ratio following massive small bowel resection. J Surg Res 91:38–42
26. Hockenbery DM, Zutter M, Hickey W, Nahm M, Korsmeyer SJ (1991) Bcl2 protein is topographically restricted in tissues characterized by apoptotic cell death. Proc Natl Acad Sci USA 88:6961–6965
27. Kamada S, Shimono A, Shinto Y, Tsujimura T, Takahashi T, Noda T, Kitamura Y, Kondoh H, Tsujimoto Y (1995) bcl-2 deficiency in mice leads to pleiotropic abnormalities: accelerated lymphoid cell death in thymus and spleen, polycystic kidney, hair hypopigmentation, and distorted small intestine. Cancer Res 55:354–359
28. Welters CF, Piersma FE, Hockenbery DM, Heineman E (2000) The role of apoptosis during intestinal adaptation after small bowel resection. J Pediatr Surg 35:20–24
29. Korsmeyer SJ, Shutter JR, Veis DJ, Merry DE, Oltvai ZN (1993) Bcl-2/Bax: a rheostat that regulates an anti-oxidant pathway and cell death. Semin Cancer Biol 4:327–332